Fast 3D velocity updates using the prestack exploding-reflector model

Claudio Guerra[1] and Biondo Biondi[2]

[1] Formerly Stanford University, Stanford Exploration Project; presently Petrobras, Brazil

[2] Stanford University, Stanford Exploration Project

Abstract

We show 3D real data results of migration-velocity analysis (MVA) by wavefield extrapolation using data synthesized by the prestack exploding-reflector model (**PERM**). PERM generalizes the exploding-reflector model (ERM) in a sense that migration of PERM data generates a prestack image. **Phase-encoding the modeling experiments** reduces drastically data size, allowing **fast MVA**. Also, since the modeling can be limited to a region with inaccurate velocity, a **target-oriented strategy** can be applied in MVA. The initial conditions for the modeling are **reflectors interpreted** in a prestack image computed by wavefield-extrapolation methods. Hence, a **horizon-based strategy** is naturally incorporated into MVA by wavefield-extrapolation.

Prestack exploding-reflector model

The fundamental idea of PERM is to synthesize areal shots whose migration describes the **correct kinematics** of a reflector in an isolated subsurface-offset common-image gather (**SODCIG**) computed with wave-extrapolation methods. This is achieved by extrapolating source and receiver wavefields starting from the prestack image at the vicinity of the SODCIG. The modeling of PERM **source** D and **receiver** U wavefields can be carried out by any wavefield-continuation scheme. Here, we use the following one-way wave equations:

$$\begin{cases} \left(\frac{\partial}{\partial z} - i\sqrt{\omega^2 s_0^2 - |\mathbf{k}|^2}\right) D(\mathbf{x},\omega;\mathbf{x_m}) = I_D(\mathbf{x_m},\mathbf{h}) \\ D(x,y,z=z_{max},\omega;\mathbf{x_m}) = 0 \end{cases}$$

and

$$\begin{cases} \left(\frac{\partial}{\partial z} + i\sqrt{\omega^2 s_0^2 - |\mathbf{k}|^2}\right) U(\mathbf{x},\omega;\mathbf{x_m}) = I_U(\mathbf{x_m},\mathbf{h}) \\ U(x,y,z=z_{max},\omega;\mathbf{x_m}) = 0 \end{cases}$$

where $\mathbf{x}$ is the spatial coordinates, $\mathbf{x_m}$ is the coordinate of the SODCIGs used in the modeling, ω is frequency, $\mathbf{h}$ is the subsurface offset, s_0 is the background velocity also used in the migration of the initial image, and I_D and I_U are prestack images used as the initial conditions for the modeling of source and receiver wavefields, respectively, and are computed by **rotating the original image** according to the apparent **geological dip**.

Using SODCIGs separately in the modeling can originate PERM data even bigger than the original data. **Combining** the modeling experiments, respecting a decorrelation distance between SODCIGs simultaneously injected, drastically decreases the imaging cost. This **decorrelation distance** is necessary to avoid **crosstalk** between unrelated wavefields and must be at least twice the subsurface-offset range. The simple model below, consisting of one reflector embedded by a constant velocity medium illustrates the correct kinematics resulting from the **3D areal-shot migration** of 48 combined PERM data (Figure 2) compared with the common-azimuth migration (**CAM**) of Figure 1.

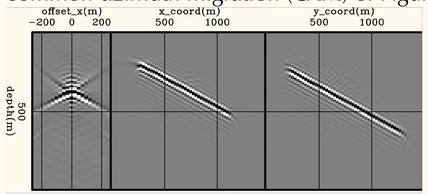

Figure 1 - Common-azimuth migration

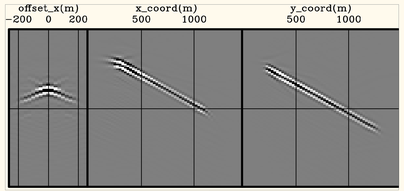

Figure 2 - Areal-shot migration of 3D-PERM data

Image-space phase-encoded wavefields

Image-space phase-encoded wavefields (**ISPEWs**) are computed using PERM along with **phase-encoding** techniques to further **improve data reduction** achieved with PERM. The phase encoding is performed during the modeling, in which the reflectors are encoded using a particular coding sequence. This allows injection of **multiple reflectors** and SODCIGs more **closely spaced** than the decorrelation distance, while diminishing the prejudicial effect of crosstalk during imaging. To be properly encoded, reflectors must be **identified in the prestack volume**. After rotation, SODCIGs are encoded according to:

$$\widetilde{I}(\widehat{\mathbf{x}},\mathbf{h},\mathbf{q},\omega) = \sum_m \sum_j \delta(\widehat{\mathbf{x}} - m\Delta\mathbf{x}) e^{i\gamma(\widehat{\mathbf{x}},j,\mathbf{q},\omega)} W_j(\widehat{\mathbf{x}},\mathbf{h}) I(\widehat{\mathbf{x}},\mathbf{h}),$$

where the delta function denotes the selection of the SODCIGs separated by the distance $\Delta\mathbf{x}$, W selects the reflector j, $\mathbf{q}$ is the realization index, and γ can be any pseudo-random sequence. Modeling of ISPEWs can be confined to a region of **velocity inaccuracy** by collecting them at its top, which allows **MVA** by wavefield extrapolation to be easily solved in a **target-oriented manner**.

Migration-velocity analysis using ISPEW

The theory of MVA by wavefield extrapolation in the **image-space generalized-sources domain** was described by Guerra et al. (2009). In this domain, PERM wavefields and ISPEW are defined and are the carriers of information in MVA. They allow **fast velocity updates** due to the small data size and to their inherent capability for being used in a target-oriented manner. These wavefields enable us to **incorporate** well-established strategies used in ray-based MVA, such as **horizon-based tomography** and possibly **grid-based tomography**, into MVA by wavefield extrapolation. This new feature gives more **flexibility** to MVA by wavefield extrapolation and can **improve convergence** to an optimal velocity.

A nonlinear conjugate gradient method is used to minimize the differential-semblance velocity analisys (DSVA) objective function (Shen and Symes, 2009)

$$J(s) = \left\| \mathbf{h}\widehat{I}_0 \right\|_2^2,$$

where $\widehat{I}_0$ is the image computed with the current velocity. To update the velocity model, we need to compute the gradient of this objective function. Figure 3 synthesizes the gradient computation using 35 ISPEWs from 12 reflectors for a portion of the Marmousi model. Velocity is to be updated only below the black line of Figure 3a, where the initial velocity is smoother and 10% slower on average than the original velocity. To mitigate illumination imperfections and provide smooth updates, the gradient is B-spline smoothed (dz=16 m dx=240 m).

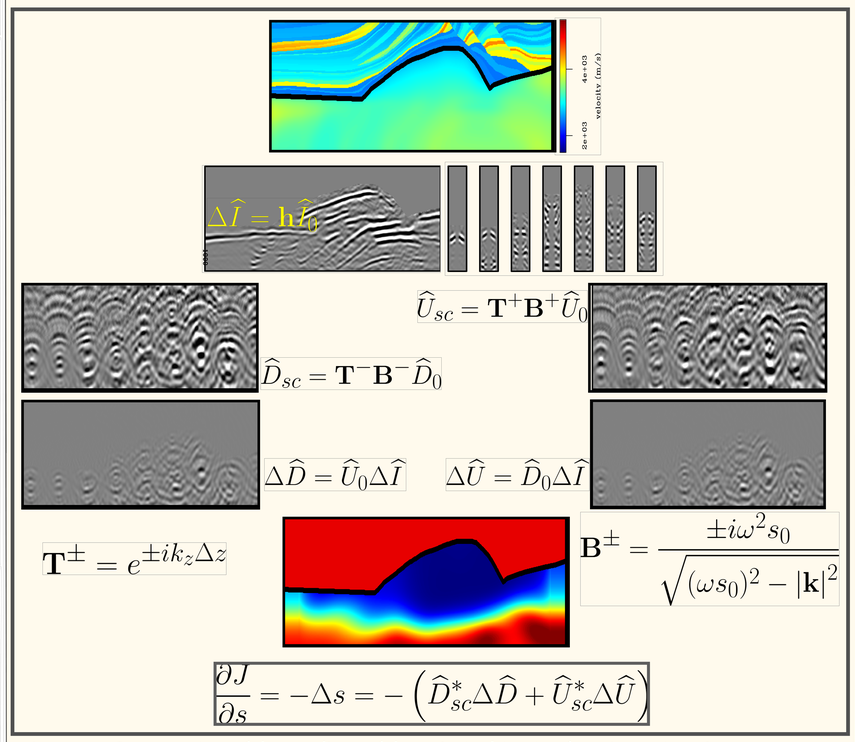

Figure 3 - Computation of the gradient of the DSVA objective function using ISPEW.

3D-Field data example

Using 3D-ISPEWs in MVA by wavefield-extrapolation is illustrated with a 3D-seismic data from the North Sea (50 km²). The challenges of this dataset for defining the velocity model are:

- a salt body with **irregular shape** and **intense faulting**
- **amplitude variations** caused by irregular acquisition
- **short offsets** (3600 m maximum) and **limited azimuths**.

Horizon-based ISWET along with salt-flooding were used in the velocity inversion, yielding consistent velocity updates, fast convergence, and a geologically plausible velocity model. Figure 4 illustrates the MVA strategy.

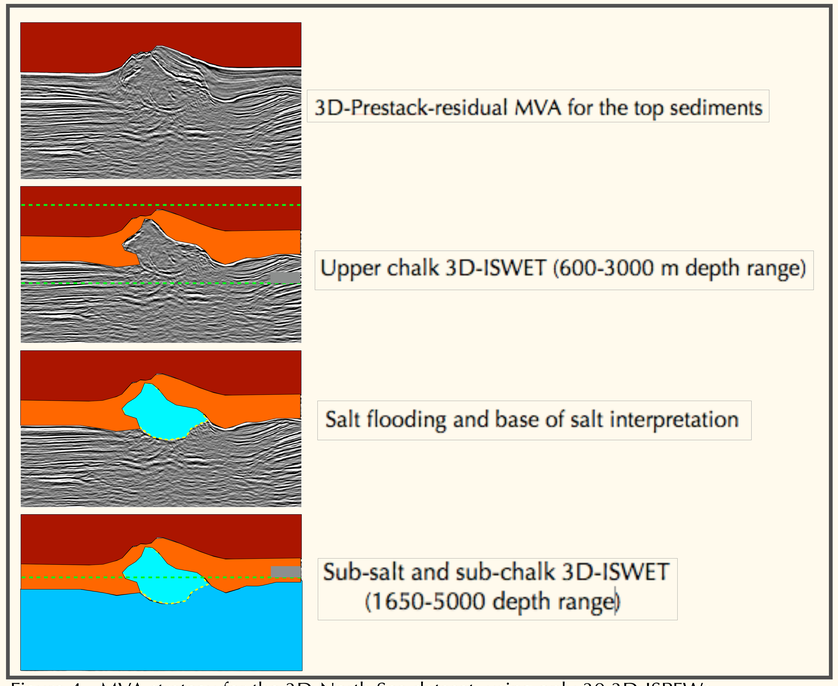

Figure 4 - MVA strategy for the 3D-North Sea dataset, using only 30 3D-ISPEWs.

The 3D dataset was submitted to azimuth-moveout (AMO), and CAM images are used as the initial conditions for the modeling of only **30 3D-ISPEWs**. SODCIGs are continuously injected in the cross-line direction since no cross-line offset is computed in CAM to model the 3D-ISPEW pair of Figure 5. This initial condition is depicted in Figure 6. For the upper chalk, only one reflector (base of chalk) is used in the modeling, whereas seven reflectors were injected to model 3D-ISPEWs for the sub-salt and sub-salt sediments.

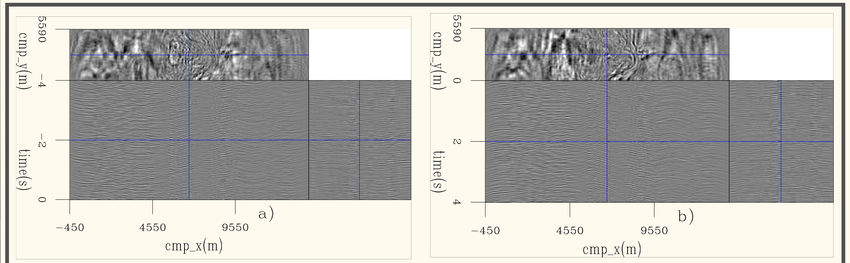

Figure 5 - 3D-image-space phase-encoded source (a) and receiver (b) data.

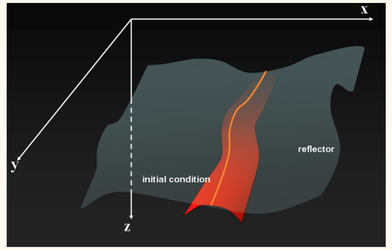

Figure 6 - CAM initial conditions for modeling 3D-ISPEW and 3D-PERM data

The initial velocity model (Figure 7a) results from refining the sediment velocity above the chalk, smoothing and scaling down 10% the velocity below the top of chalk of an available velocity model defined using a ray-based method. The final velocity model (Figure 7b) was obtained after seven iterations of nonlinear conjugate gradients using the MVA strategy of Figure 4.

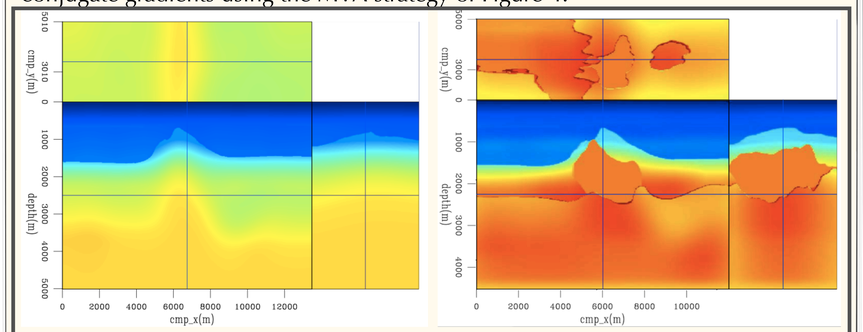

Figure 7 - Initial velocity model (a) and final velocity model (b)

CAM images computed with the velocity models of Figure 7 and with the velocity model defined with a ray-based method are sown in Figure 8. It is clear the **better focusing** of the reflectors, **imaging of faults**, and definition of the **salt body contours** of the image computed with the final velocity model (Figure 8c and 9c) compared to that using the initial velocity model (Figures 8a and 9a) and the original velocity model (Figures 8b and 9b).

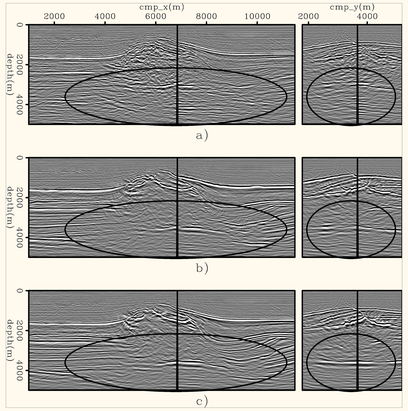

Figure 8 - CAM images using the initial (a), the original (b), and the final (c) velocity.

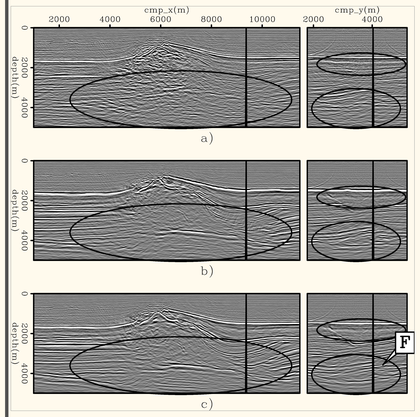

Figure 9 - CAM images using the initial (a), the original (b), and the final (c) velocity.

Conclusions

The **computational efficiency** and **flexibility** achieved with **PERM** data and **ISPEW** enables the use of **migration-velocity analysis by wavefield extrapolation** as a **routine procedure** to define the 3D-migration-velocity model in areas of complex geology. 3D-field data examples show that **accurate velocity** models are obtained at a **low cost**.

Aknowledgements

The authors would like to thank the sponsors of the Stanford Exploration Project for the financial support and TotalFinaElf for providing the field data. Claudio Guerra is indebted with Petrobras for all the support during his PhD.

References and further reading

Guerra, C., Y. Tang, and B. Biondi, 2009, Wave-equation tomography using image-space phase encoded data: SEG Technical Program Expanded Abstracts, 28, 3964– 3968.

Guerra, C., 2010, Migration-velocity analysis using image-space generalized wavefields, PhD thesis, Stanford University.

Shen, P. and W. W. Symes, 2008, Automatic velocity analysis via shot profile migration: Geophysics, 73, VE49–VE59.

BR PETROBRAS